

A Reliable Night Vision Image De-Noiseing Based on Optimized ACO-ICA Algorithm

Jingjing Ren

Abstract—Due to the intricate nature of nocturnal working environments, real-time night vision images often exhibit a considerable degree of noise. This noise significantly hampers the precision of image processing systems responsible for recognition tasks. This study focuses on the enhancement of night vision image quality by addressing the issue of noise. Initially, we utilize the difference image method to analyze various sources of noise. Our findings unequivocally identify a mixed nature of noise, with a significant presence of Gaussian noise. Subsequently, we employ the Independent Component Analysis (ICA) algorithm to reduce the Gaussian noise component. To overcome the inherent limitations of the ICA algorithm, such as susceptibility to local minima entrapment and slow convergence, we apply the Ant Colony Optimization (ACO) algorithm to optimize the ICA. This combination results in the development of the ACO-ICA de-noising algorithm. In a series of simulation experiments, the ACO-ICA algorithm is compared with conventional median filtering and the standalone ICA approach, demonstrating that the ACO-ICA algorithm outperforms the other methods significantly. This difference is statistically significant at a significance level of 0.05, highlighting the substantial variation in de-noising effectiveness among the three approaches. In terms of visual impact, the ACO-ICA algorithm effectively reduces noise, leading to a noticeable improvement in edge delineation. Quantitative evaluation using the Relative Peak Signal-to-Noise Ratio (RPSNR) further validates the superiority of the ACO-ICA de-noising strategy. When compared to the original night vision image, median filtering, and ICA de-noising, the ACO-ICA denoised image demonstrates an average RPSNR increase of 20.28%, 12.25%, and 4.60%, respectively. Notably, the use of an incandescent lamp as an artificial light source yields the most favorable de-noising results.

Index Terms—night-vision image; ICA; ACO-ICA de-noising algorithm; relative peak signal-to-noise ratio

I. INTRODUCTION

ALONG with the progress of science and the development of industrial technology, the development of agricultural robot technology has become increasingly more mature [1], and the concurrent development level of apple harvesting robots has reached an unprecedented height [2]. The work of apple harvesting is strongly seasonal, labour intensive and inefficient. To further liberate the agricultural labour force, improve production efficiency, and reduce economic loss, a night-time apple harvesting robot is proposed in this study, which will address maximum utility. Currently, relatively little research has been done on nighttime[3]. Due to working

at night, the acquired real-time night vision images contain an abundance of noise, which is caused by light, temperature, humidity and other factors. They influence the operating efficiency and precision of the image recognition system, which affects the efficiency of apple harvesting robots during the harvest process. Therefore, to realize an optimal night-time apple harvesting robot, the de-noising process of real-time apple harvesting night vision imaging needs to be considered. Regarding the determination of the specific category of noise present in night vision imagery, there is no good method. In previous studies on night-vision imaging, it was assumed that the noise is dominated by Gauss noise [4, 5], and the Gauss noise is more common in the image. To better ascertain the type of noise, this study attempts to introduce the difference imaging method. Based on the analysis of two images that are acquired in the same conditions and the same sample points, the type of the noise is determined.

Gauss noise widely exists in sound, images, electromagnetic waves and other signals, but how to reduce Gauss noise is still a problem [6, 7]. Therefore, many scholars have conducted studies on de-noising Gauss noise, in which many de-noising algorithms have been proposed in many fields and achieved good results [8, 9], but studies of night vision image de-noising are remain scarce [10]. Thus, in the field of practical applications, there is space for further improvement in the de-noising effect of Gauss noise and the details of the signal process. In this study, we propose the utilization of independent component analysis (ICA) [11] in the de-noising algorithm to enhance the reduction of noise pollution in night vision images. ICA is the earliest and most extensively used approach for separating blind signal[12]. It has been become a research topic of interest in the field of signal processing and is used in image compression, feature extraction, de-noising and other aspects. It is an analysis method based on the high-order statistical characteristics of the signal, which can more fully reveal the essence of the structure in image processing. Under certain conditions, ICA is used to extract the signal originating from the image source in noise contaminated images, achieving the effect of denoising[13]. The ICA de-noising algorithm has been widely used in many fields, such as medical imaging [14], engineering technology [15] and so on, and has achieved a relatively ideal de-noising effect [16, 17].

In recent years, ICA applications have made notable achievements. However, with the gradual deepening of ICA research, a series of problems have been exposed, such as iterative calculations, easily falling into local minima, slow convergence speed and so on. These factors lead to a decrease in the operating efficiency of ICA, and the final result is not ideal. Therefore, many optimized algorithms have been

Manuscript received May 3, 2023; revised December 13, 2023.

This work is supported by Teaching Reform and Innovation Project of Higher Education Institutions of Shanxi Province (J20221194); Shanxi Education Science "14th Five-Year Plan" Project (GH21607).

J. Ren is lecturer of Department of Intelligence and Automation, Taiyuan University, Taiyuan 030032, China (e-mail: 511924532@qq.com)



Fig. 1. Original apple image under different lighting environment. Form left to right, (a) Natural light, (b) Incandescent light, (c) Fluorescent light, (d) LED light

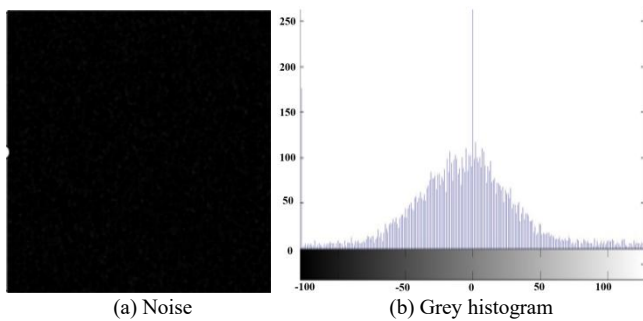


Fig. 2. Diagram of difference imaging. From left to right

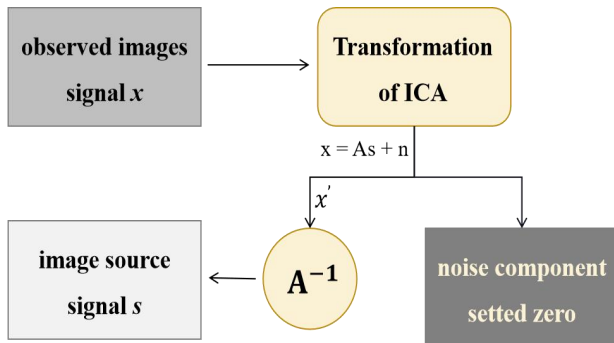


Fig. 3. Flow chart of ICA de-noising

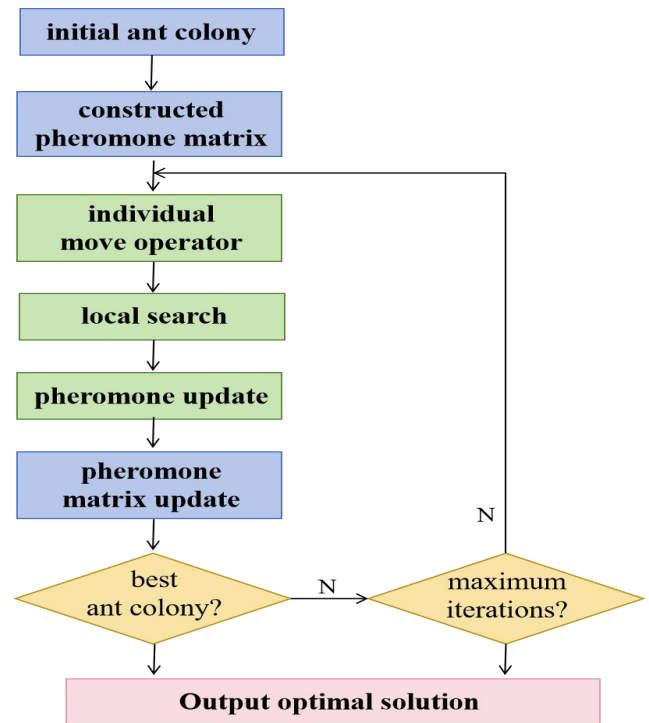


Fig. 4. Flow chart of ACO algorithm

proposed by scholars and have yielded favorable outcomes. In this study, the ant colony optimization (ACO) algorithm is introduced, which is a type of swarm intelligence and global optimization algorithm [18]. The solution of the ICA separation matrix is optimized by ACO in order to improve the operating efficiency and separating effect of the ICA, resulting in an optimized ICA algorithm based on ACO (ACO-ICA). The new ACO-ICA algorithm is employed for reducing noise pollution in night vision image de-noising.

This study focuses on investigating the feasibility of continuous operations for apple harvesting robots. The study involves capturing night vision images of apples within an orchard setting. Different artificial light sources are employed as auxiliary lighting during nighttime operations. Initially, the noise present in the apple night vision images is meticulously examined using the difference imaging method. This analysis serves the purpose of identifying the specific

type of noise affecting these images. Subsequently, the ICA is introduced to facilitate the de-noising of the night vision images. In order to enhance operational efficiency, the ACO algorithm is employed to optimize the image processing. As a culmination of these steps, an advanced de-noising approach named ACO-ICA is formulated, which harnesses the optimized ICA process for enhancing the quality of night vision images. To verify the operating efficiency and de-noising performance of the new algorithm, a simulation experiment is set up using the apple natural light image to conduct testing. Noise is added into the two respective images, and then a median filter is used. The FastICA is used to de-noise and compare the results with the ACO-ICA algorithm. The visual effect, peak signal-to-noise ratio, and running time are used to evaluate the de-noising performance of each de-noising algorithm, and significance tests are performed. The new algorithm is applied to de-noise night

vision image noise, and the experiments are repeated many times. The visual effect, edge details, relative peak signal-to-noise ratio, and running time are used to evaluate the experimental results. Subsequently, the most suitable artificial light source is selected for working at night.

II. NIGHT VISION IMAGE ACQUISITION AND NOISE ANALYSIS

A. Night vision image acquisition

Under several different light environments and from many sampling points, natural light images and night vision images of apples are acquired. The details of the image acquisition process are as follows.

Image acquisition site: Dashahe apple production park, Feng country, Jiangsu province, China. Light environment: The night environment is the reference for when the test illuminance of natural light is below 1 lx. Natural light is a reference to that general light environment.

Artificial light source: An incandescent lamp (DC 12 V, 35 W), a fluorescent lamp (DC 12 V, 35 W), and an LED lamp (made up of 9 groups of 1 W with aluminium plate beads, arrange) with the power supplied by a lead-acid battery (12 V, 36 Ah). Image acquired method: The sampling points are marked from the same position and angle to acquire images.

As shown in Figure 1, four different apple images are acquired by the same acquisition angle from one point. Respectively, these encompass natural light, the incandescent lamp, the fluorescent lamp and the LED lamp environments.

B. Visual analysis

In this study, we employ difference image analysis to discern the type of noise present in night vision images. The underlying principle of this method hinges on the randomness of noise generation and distribution. In a uniform sampling environment, when two images are captured from a single sampling point, taking the instance of acquiring night vision images of apples under an incandescent lamp, the absence of noise is indicated by a resulting difference image with all corresponding pixel points having a grey value of 0, as illustrated in Figure 2. Conversely, if noise is present, the grey value at the corresponding pixel point will deviate from 0, thus identifying it as noise data. The application of differential image analysis to the acquisition of night vision images, exemplified by the scenario of capturing apple images under an incandescent lamp, is depicted in Figure 2 for clarity.

Figure 2 presents the subtraction result derived from the two night vision images in Figure 2(a), with the corresponding grey histogram depicted in Figure 2(b). Notably, the grey histogram distribution closely resembles a Gaussian distribution. This observation leads to the inference that the predominant noise category in the night vision images is Gaussian noise.

Similarly, the differential image analysis method is applied to analyze the other two variations of night vision images, yielding consistent results through repeated experiments. Consequently, the noise type in apple night vision images is conclusively identified as mixed noise, with a predominant presence of Gaussian noise, albeit with some instances of salt and pepper noise.

III. ACO-ICA DE-NOISING ALGORITHM

Given that the primary type of noise present in night vision images is Gauss noise, it remains a challenging problem to resolve at present. This study integrates ICA into the night vision image de-noising algorithm. To overcome the defects of the ICA algorithm, such as easily falling into local minima, a slow convergence speed, and so on, ACO attempts to optimize the process. The separation matrix of ICA is optimized by ACO, and an optimized ICA de-noising algorithm based on ACO is established (ACO-ICA).

A. ICA de-noising algorithm

The fundamental principle behind ICA de-noising is considering the noisy image as a composition of two independent signals, namely, the image source signal and the noise signal. ICA image de-noising is used as a reference to separate the source signal and noise signal of the observed signal and achieve the purpose of de-noising. In this way, this method can reduce detail loss. Figure 3 depicts the flowchart of the ICA de-noising algorithm.

Suppose the noisy ICA model is expressed as follows:

$$x = As + n \quad (1)$$

where x is the observed image signal, $s = [s_1, s_2, \dots, s_n]^T$ is the source image signal, $n = [n_1, n_2, \dots, n_m]^T$ is the noise signal, $n \sim N(0, \sigma^2)$, A is an $m \times n$ hybrid matrix, and s and n are independent of each other.

The maximum likelihood method is used to estimate the mixture matrix. However, in the noisy ICA model, simply estimating the mixture matrix is insufficient. Therefore, we reverse formula (1) as

$$Wx = s + Wn \quad (2)$$

where W is the separation matrix. The obtained independent components contain the noise estimation. In fact, we expect that the obtained estimation is the source signal independent component \hat{s}_i , and we make this component reach its optimum to a certain extent, which contains the minimum noise. The essential stages of the ICA de-noising algorithm involve the following steps:

Step 1 Utilize the noise-free training set u to estimate the base vector of ICA, $u = As$, obtain the estimates of A , namely, \hat{A} , sets $W_0 = \hat{A}^{-1}$, and utilizes $W = W_0(W_0^T W_0)^{-\frac{1}{2}}$;

Step 2 Estimate the probability density of each component $s_i = w_i^T u$ and then estimate \hat{X} of the observed noisy signal using the ICA transform to calculate sparse transform projection $Y = W\hat{X}$;

Step 3 Use the maximum likelihood contraction function g_i to de-noise estimate s_i , namely, $s_i = g_i(y_i)$; and

Step 4 Invert the ICA transformation and then obtain the low-noise image estimation $\hat{X} = W^T \hat{S}$.

B. ACO-ICA algorithm

ACO is a type of bionic evolution and swarm intelligence heuristic search algorithm, which uses information exchange and mutual cooperation between individuals to solve complex optimization problems. It is applicable to both local optimization and global optimization. The ACO algorithm has many advantages, such as robustness, parallelism, positive feedback, discreteness, and so on. It has proven to be effective in resolving combinatorial optimization problems and has gained widespread adoption in various fields. The ACO algorithm is an iterative operation, and its algorithm

flow is shown in Figure 4. It simulates the foraging behavior of ants, where ant colonies transmit information between individuals and search for the shortest path from ant nests to food. The feasible solution of each optimization problem is regarded as an ant in the search space. After each ant executes a movement operator, it evaluates the overall population, records the optimal ant, and then updates the pheromone matrix based on the information mutual update operator to complete an iteration. That is, each candidate solution continuously adapts its own structure in response to the gathered information, and communicates with other candidate solutions through information to generate the optimal solution.

The traditional ICA algorithm mostly uses the gradient optimization method, which creates some disadvantages. Therefore, when ICA is applied to image processing, the phenomena of a long running time and incomplete de-noising easily occur. Considering these problems, this study uses ACO for the optimization. The core of the ICA algorithm lies in solving the separation matrix. Namely, separation matrix W of formula (2) is solved by ACO optimization, which can enhance the precision and efficiency of the de-noising algorithm.

Assuming the number of ant colonies is N , the probability of the ant K transitioning from position i to j at time t is defined by formula 3:

$$p_{ij}^k = \frac{\tau_{ij}^\alpha(t)\eta_{ij}^\beta(t)}{\sum_{j=1}^q \tau_{ij}^\alpha(t)\eta_{ij}^\beta(t)} \quad (3)$$

In which, τ_{ij} represents the residual information amount of the i - j connection at time t , and η_{ij} denotes the anticipated level of ant movement from position i to j , usually taken as $\eta_{ij} = 1/d_{ij}$. d_{ij} represents the distance from position i to j , α is the information heuristic factor, β is the expected heuristic factor, and q represents the count of positions that the ant k can select in the subsequent step. To prevent residual information from obscuring heuristic details, it is essential to update the residual information after each ant completes a single step. The update equation is formulas 4 and 5:

$$\tau_{ij}(t+1) = (1-\rho)\tau_{ij}(t) + \Delta\tau_{ij} \quad (4)$$

$$\Delta\tau_{ij} = \sum_{k=1}^N \Delta\tau_{ij}^k(t) \quad (5)$$

In which, ρ is the attenuation coefficient of mutual information, $\Delta\tau_{ij}$ is the increment of pheromones, and $\Delta\tau_{ij}^k(t)$ is the amount of information left by the k -th ant in this cycle. In the formula 6, Q is a constant, and L_k is the length of the path traveled by the k -th ant in this loop.

$$\Delta\tau_{ij}^k = Q/L_k \quad (6)$$



Fig. 5. Resulting image with added noise

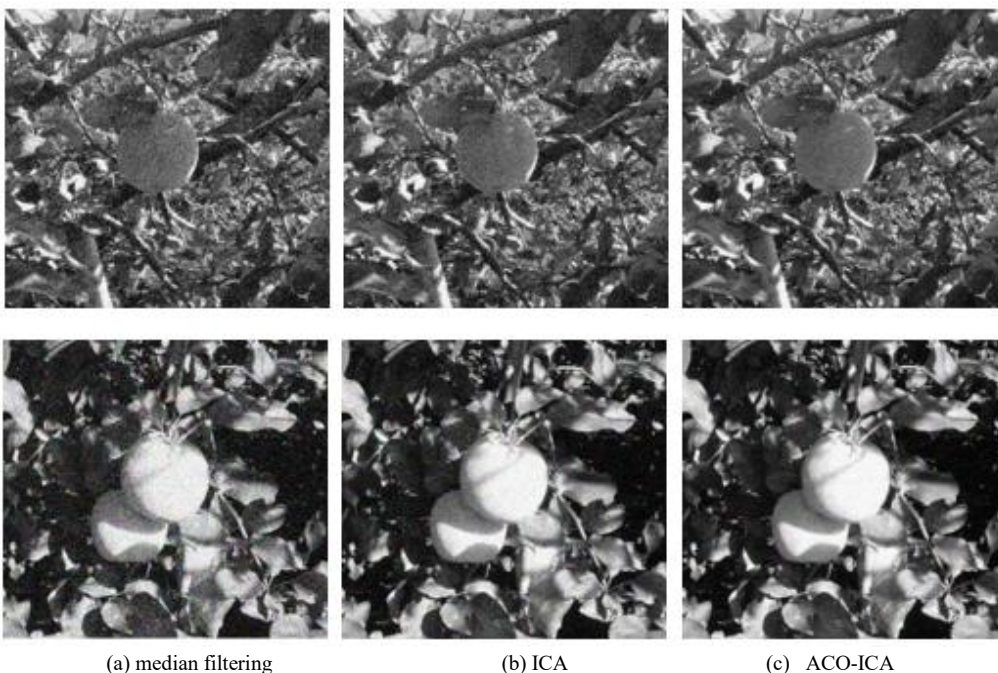
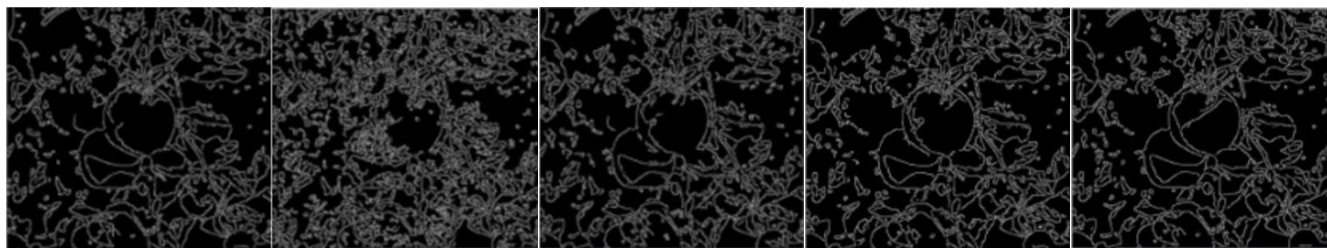


Fig. 6. Effect comparison of the three de-noising methods



(a) Original images (b) Added noise (c) Median filtering (d) ICA images (e) ACO-ICA images
Fig. 7 Effect comparison of canny edge detection

TABLE I PSNR OF THE LOW NOISE AND ADDED NOISE IMAGE

Image	Added noise image	Median filtering	ICA	ACO-ICA
Single fruit image	30.0263	31.6729	34.3037	36.2846
Two fruits image	30.8147	32.3145	35.1477	37.0153

TABLE II ANALYSIS OF VARIANCE FOR THE THREE DE-NOISING ALGORITHMS

Source of variance	SS	DOF	MS	F
Factors	46.3315	3	15.4438	54.2012
Error	1.1397	4	0.2849	
Total	47.4712	7		

Note: SS refers to the sum of square, DOF is degrees of freedom, and MS denotes mean square.

TABLE III ANALYSIS OF VARIANCE FOR THE THREE DE-NOISING ALGORITHMS

Image environment	original image	Median filtering	ICA	ACO-ICA
Incandescent light	29.1873	31.6231	33.6718	36.2228
Fluorescent light	28.6315	30.2046	32.6673	33.8961
LED light	27.9092	30.0284	32.2360	33.0335

Ant colony intelligence is used to optimize the separation matrix W . Initially, we set the value range of the separation matrix such that each component value of separation matrix is limited. In this study, we set $-1 \leq w_{ij} \leq 1$, and this range is divided into several intervals in order to conduct ant colony optimization on a global scale. Each interval is dynamically divided into sub-intervals in order to ensure the local optimization of the ant colony. The separation matrix is processed by orthogonalization.

First initialize the ant colony. The ant colony is used to express the separation matrix; the ant colony is placed into each interval randomly, and the initial pheromone τ_0 of each interval is set. The ant colony carries out the random search in the initial interval, and with the pheromone update, the ant can move to the better solution. The fundamental steps of the ACO-ICA de-noising algorithm involve the following procedures:

Step 1 The observation signal x is centralized, and the whitening process occurs;

Step 2 Set the range of the separation matrix W and divide it into N intervals;

Step 3 Initialize the ant colony and pre-set the number of ants, the volatilization coefficient of the pheromone, the initial residual information, and so on;

Step 4 All ants are uniformly distributed into the N solution space;

Step 5 According to formula (3), each ant moves to the interval that has the maximum transition probability;

Step 6 To calculate the objective functional value and conduct the local and global optimization, select the optimal solution and turn to step 8; otherwise, turn to step 7;

Step 7 According to formulas (4) and (6), update global pheromone and return to step 5; and

Step 8 Output the optimal solution if the maximum number of iterations has been reached, namely, the optimal generation of the ant colony corresponding to the separation matrix. Otherwise, return to step 5.

The ACO-ICA algorithm can optimize the relatively ideal separation matrix W , and it can be applied to image de-noising. From section 3.1, the highest estimates of the source signals can be obtained from the observed image, which means that the low-noise image is obtained.

IV. SIMULATION EXPERIMENT

To better verify the de-noising performance of the ACO-ICA algorithm, the simulation experiment is arranged in this study. Two natural light apple images are selected. For

these two images, respectively, we add $\sigma_n^2 = 0.05$ Gaussian noise and $P = 0.05$ salt and pepper noise, as shown in Fig. 5.

To validate the effectiveness of the newly proposed method, this study employs median filtering, the FastICA (in the following, it is called the ICA), and ACO-ICA, and the three de-noising algorithms are compared. The basic parameters of each de-noising algorithm settings are as follows: the median filtering method uses a window size of 3×3 , the FastICA method uses an orthogonal transformation using an 8×8 base graph, and the ACO-ICA de-noising method uses $N = 100$, $\rho = 0.1$, $\alpha = 1$, $\beta = 5$, and $Q = 1$, and the maximum number of iterations is 100.

A. Visual effect and edge detection

After the three de-noising algorithms are applied to address the two added noise images, the low-noise images are shown in Figure 6.

From the visual observation of Figure 6, compared with median filtering and the ICA de-noising algorithm, the new ACO-ICA de-noising algorithm is relatively optimal. The low-noise image produced by the new algorithm exhibits the fewest noisy points and is the clearest.

Direct visual observation often suffers from subjectivity. To objectively assess the performance of each de-noising algorithm and further investigate the detailed information of the image, image edge detection is conducted. This study selects the Canny edge detection operator, which is the most commonly used method and has excellent performance. Taking one picture as an example, the edge detection effect picture of the natural light apple image is shown in Figure 7.

As depicted in Figure 7, the contour details of the low-noise image are extracted through edge detection, elucidating the pronounced impact of noise on the image. Notably, the outcome of the ACO-ICA de-noising algorithm yields a low-noise image that remarkably resembles the original. This is particularly evident in the preservation of intricate image edge nuances and textural intricacies. The juxtaposition of these Figure 7 (c)(d)(e) unequivocally highlights the superior noise reduction capability of the ACO-ICA algorithm, underscoring its efficacy in retaining essential visual details.

B. PSNR and significance test

The evaluation of the visual effect and edge detection often has some subjective factors. In order to assess the de-noising effect more objectively, we also compute the peak signal-to-noise ratio of the low-noise image. The results of this evaluation are presented in table 1.

Table 1 presents a quantitative comparison of the three distinct de-noising algorithms based on objective numerical metrics. Following the de-noising procedures, the PSNRs of the resultant low-noise images are computed. Notably, the PSNR achieved through median filtering is the least favorable when contrasted with the other two methods. In comparison, the application of the ICA de-noising technique exhibits a considerable enhancement in PSNR, showcasing a marked improvement over the median filter approach.

To provide further elucidation on the effectiveness of the novel de-noising algorithm, difference testing is required for the PSNR values of three de-noising algorithms. According to the PSNR results from table 1, the outcomes of the

variance analysis are presented in table 2.

$F_{0.05}(3,4) = 6.59 < 54.2012$, and at the 0.05 significance level, it is determined that the PSNRs of three de-noising algorithm are significantly different.

Collectively, the outcomes consistently highlight the exceptional quality of the low-noise images generated through the implementation of the ACO-ICA de-noising algorithm. This superiority is apparent whether one evaluates the results through visual appraisal or quantitative analysis utilizing the PSNR values. Remarkably, the ACO-ICA de-noising algorithm adeptly preserves intricate image characteristics such as edge delineation and textural nuances.

V. NIGHT VISION IMAGE DE-NOISING EXPERIMENT

A. Experimental preparation

Under normal circumstances, we evaluation of the de-noising effect mainly from three aspects: the visual effect, the signal-to-noise ratio and the running time. For the evaluation of the visual effect, a large visual gap can lead to an effective qualitative judgement, but it cannot be used for a quantitative comparison. If the gap is not too obvious, a visual qualitative judgement will also be relatively difficult. Visual evaluations contain very strong subjectivity, vary from person to person, and people can obtain different conclusions. Therefore, it is difficult to achieve an objective and fair visual evaluation.

To more objectively evaluate the de-noising effect of each de-noising algorithm using a numerical value, we calculate the signal-to-noise ratio that needs a noise-free image as a benchmark. This study attempts to propose the concept of the relative peak signal-to-noise ratio (RPSNR), which is defined as follows.

Consistent with the acquired natural light images being the benchmarks (regarded as noise-free images), they are considered as the original noise-free image signal. A natural light image is considered as the signal reference of other pending night vision images, and the calculated peak signal-to-noise ratio is defined as the relative peak signal-to-noise ratio of the low-noise image or the night vision image. In the calculation process, natural light images are used as unified benchmark references for several night vision images. Namely, they use the same reference and the same calculation standards so that the results are comparable. The RPSNR from the view of providing a numerical value is used to objectively evaluate the de-noising effect. Its expression is

$$RPSNR = 10 \lg \left[\frac{255^2}{\frac{1}{MN} \sum \sum (u_{ij} - l_{ij})^2} \right] \quad (7)$$

where MN represents the number of pixels in the image, u_{ij} is the grey value of pixel (i, j) on the night vision image or low-noise image, and l_{ij} is the grey value of pixel (i, j) on the natural light image.

B. Night vision image de-noising

We use the three de-noising algorithms of the median filter, ICA and ACO-ICA to address the noisy apple night vision images, which were acquired under three artificial light environments. Figure 8 illustrates the comparison of the de-noising effects.

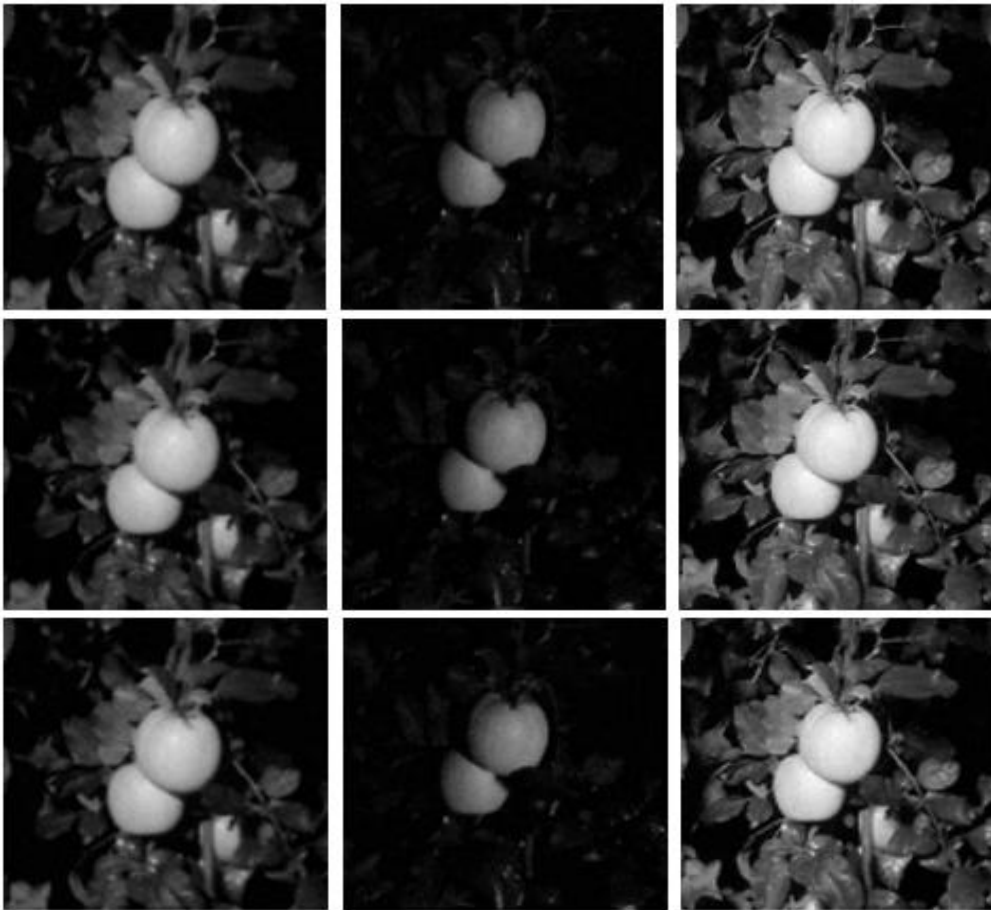


Fig. 8. Effect comparison of the three de-noising methods, from left to right is Incandescent light, Fluorescent light, LED light; from up to down is median filtering, ICA, ACO-ICA.

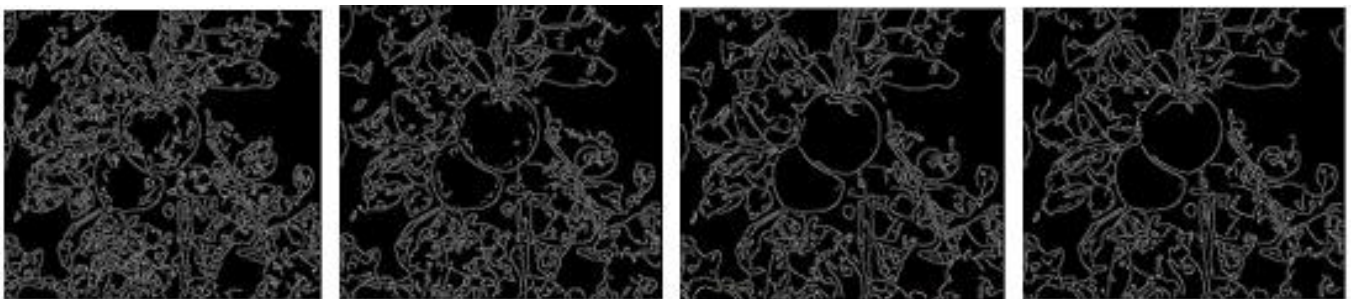


Fig. 9. Canny edge detection of incandescent light images, from left to right is (a) Original, (b) Median filtering, (c) ICA, (d) ACO-ICA

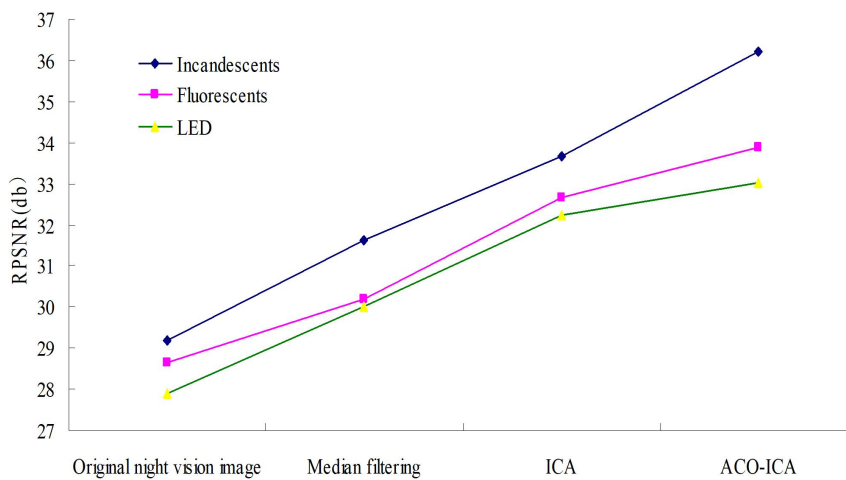


Fig. 10. Trend chart of de-noising effects

Using the image of incandescent light as an example, the results for the original night vision image and low-noise images determined by edge detection are shown in Figure 9.

To overcome the subjective factors of visual evaluation and more intuitively show the de-noising ability of the three algorithms, we further calculate the RPSNR of the low-noise images, and outcomes are detailed in table 3. It is evident that regardless of the image environment, the PRSNR of ACO-ICA is higher than median filtering and ICA.

C. Experimental results and analysis

Visual intuition is a direct visual evaluation of the low-noise image processed by the de-noising algorithm, and this is standard to a certain extent based on the subjective sense of the individual. The valuation of the objective data adopts the relative peak signal-to-noise ratio, which is a numerical, objective measure.

Visual and edge information evaluation

From Figures 2 and 8, the three de-noising algorithms contribute to a certain degree of noise reduction in night vision images. Upon comparing the low-noise images, it seems that the de-noising effect of the median filtering algorithm is comparatively inferior. There are more residual noise points and the image not clear, which means that the de-noising effect is not complete. Compared with median filtering, the low-noise image derived from the ICA de-noising algorithm is clear, but there are still many noisy points that need to be further improved. In comparison to the other two de-noising methods, the ACO-ICA de-noising effect is the best. The image with low-noise is the clearest, and it has the fewest noise points. The ACO-ICA de-noising algorithm significantly enhances the quality of image restoration, thereby greatly improving the visual quality as well. Nonetheless, with certain subjective factors, it remains challenging to objectively evaluate the real de-noising effect.

From Figure 9, with respect to the extracted edge information of the four images, based on their overall outline, the low-noise image obtained through the ACO-ICA de-noising algorithm exhibits the highest clarity. It clearly observes the textures, edges, and other detailed information of images. Similarly, with respect to the other two types of night vision images that perform edge detection, the results of other artificial lights are consistent with incandescent lights. This indicates that the ACO-ICA de-noising algorithm is the most conducive to extracting detailed information.

Numerical evaluation

As seen in Table 3, from the view of using numerical values to evaluate the de-noising effects, compared with median filtering, the ICA's and ACO-ICA's corresponding RPSNRs show greater improvements. Compared with ICA, the ACO-ICA's corresponding RPSNR still shows some improvement. With respect to the de-noising capabilities of three de-noising algorithms, their trends are consistent with the previous simulation experimental results.

To more intuitively observe the de-noising effect with respect to the broken line graph drawn using the RPSNR values of table 3, we can clearly observe the de-noising ability of each de-noising algorithm, as shown in Figure 10.

Artificial light source evaluation

To more intuitively observe the effect of an artificial light

source on night vision images, a histogram is drawn using the RPSNR values of table 3. This clearly illustrates the de-noising ability of each de-noising algorithm under different artificial light sources, and the effect is shown in Figure 10.

Analyzing Figure 10 in detail reveals insightful distinctions among the night vision images captured under three distinct artificial light sources. Particularly, when juxtaposed with the RPSNR values of the initial night vision images, the incandescent light source exhibits the highest RPSNR value. This signifies that it possesses the least amount of noise among the considered sources. Notably, the trend persists even after the application of the de-noising procedures, with the RPSNR of the incandescent lighted image maintaining its premier position. This consistent superiority in RPSNR underscores the evident effectiveness of the de-noising process on images illuminated by the incandescent light source. As a result, a compelling conclusion can be drawn: the incandescent lamp emerges as the most suitable choice for deployment as the auxiliary artificial light source for the apple harvesting robot. This strategic selection is poised to significantly bolster the subsequent stages of image recognition, promising enhanced performance and accuracy in the robotic system's operations.

VI. CONCLUSION

This paper uses night vision images obtained under various artificial light sources. A series of related studies is gradually carried out, and the first concern is the problem of night vision image de-noising. Regarding night vision image acquisition, in the apple orchard, under the three different light environments of incandescent, fluorescent and LED lights, many groups of night vision images are acquired. Difference image analysis is applied to identify the noise types, revealing that the apple night vision images consist of mixed noise, predominantly comprising Gaussian noise with some instances of salt and pepper noise.

In view of the noise characteristics of night vision images, the study introduces the ICA algorithm into the de-noising process. ACO is used to overcome the defects of ICA, such as being easily trapped in local minima, slow convergence, and so on. Therefore, an optimized ACO-ICA de-noising algorithm is further established. The simulation experiment adopts the standard Lenna image and the apple natural light image for testing. The results demonstrate that the new algorithm surpasses median filtering and ICA in terms of its de-noising ability, operating efficiency and detail information, and there are significant differences in the ability of the three de-noising algorithms. The results indicate that the ACO-ICA algorithm demonstrates the most superior performance in terms of its intuitive visual feel, detailed edge information, objective RPSNR values, and running time. Regarding the artificial light source selection, the night vision image captured under incandescent light performs better, indicating its suitability as an auxiliary light source for the apple harvesting robot.

REFERENCES

- [1] Bac, C. W., van Henten, E. J., Hemming, J., & Yael, E. (2014). Harvesting robots for high-value crops: state-of-the-art review and challenges ahead. *Journal of Field Robotics*, 31(6): 888-911.

- [2] Zhao D. A., Lv, J. D., Ji, W., Zhang, Y., & Chen Y. (2011). Design and control of an apple harvesting robot. *Biosystems Engineering*, 110: 112-122.
- [3] Han, J., Yue, J., Zhang, Y., & Bai, L. F. (2014). Salient contour extraction from complex natural scene in night vision image. *Infrared Physics & Technology*, 63: 165-177.
- [4] Camarena, J. G., Gregori, V., Morillas, S., & Sapena, A. (2013). A simple fuzzy method to remove mixed Gaussian-impulsive noise from color images. *IEEE Transactions on Fuzzy Systems*, 21(5): 971-978.
- [5] Swee, S., Chen, L., Chiang, T. and Khim, T. (2023). Deep convolutional neural network for SEM image noise variance classification. *Engineering Letters*, 31(1): 328-337.
- [6] Saba, T., Rehman, A., Al-Dhelaan, A., & Alrodhaan, M. (2014). Evaluation of current documents image denoising techniques: a comparative study. *Applied Artificial Intelligence*, 28(9): 879-887.
- [7] He, X., Wang, Y. and Yang, S. (2022). Gaussian mixture CBMeMBer filter for multi-target tracking with Non-Gaussian noise. *IAENG International Journal of Applied Mathematics*, 52(3): 568-575.
- [8] Payne, A. B., Walsh, K. B., Subedi, P. P., & Jarvis, D. (2013). Estimation of mango crop yield using image analysis–Segmentation method. *Computers and Electronics in Agriculture*, 91: 57-64.
- [9] Chan, W. and Sim, K. (2021). Termination factor for iterative noise reduction in MRI images using histograms of second-order derivatives. *IAENG International Journal of Computer Science*, 48(1): pp174-180.
- [10] Yang, S. B., He, X., Cao, H., & Cui, W. (2011). Double-plateaus histogram enhancement algorithm for low-light-level night vision image. *Journal of Convergence Information Technology*, 6(1): 251-256.
- [11] Oliveira, P. R., Morimitsu, H., & Tuesta, E. F. (2010). Using visual metrics to selecting ICA basis for image compression: a comparative study. *Lecture Notes in Artificial Intelligence*, 6433: 80-89.
- [12] Yang, S. M., Yi, Z., & Liu, G. S. (2007). Regression ICA algorithm for image denoising. *1st International Conference on Cognitive Neurodynamics*, 993-997.
- [13] McKeown, M. J., Wang, Z. J., Abugharbieh, R., & Handy, T. C. (2006). Increasing the effect size in event-related fMRI studies. *IEEE Engineering in Medicine and Biology Magazine*, 25(2): 91-101.
- [14] Sardouie, S. H., Shamsollahi, M. B., Albera, L., & Merlet, I. (2015). Interictal EEG noise cancellation: GEVD and DSS based approaches versus ICA and DCCA based methods. *IRBM*, 36(1): 20-32.
- [15] Chang, A. C. (2015). Using ICA to improve blind subspace-based channel estimation for OFDM system under unknown noise fields. *AEU-International Journal of Electronics and Communications*, 69(1): 449-454.
- [16] Ding, W. (2011). A new method for image noise removal using Chaos-PSO and nonlinear ICA. *International Conference on Advances in Engineering*, 24: 111-115.
- [17] Nath, M. K., & Dandapat, S. (2013). Multiscale ICA for fundus image analysis. *International Journal of Imaging Systems and Technology*, 23(4): 327-337.
- [18] Tavares, N. R., & Godinho, F. M. (2013). Literature review regarding Ant Colony Optimization applied to scheduling problems: Guidelines for implementation and directions for future research. *Engineering Applications of Artificial Intelligence*, 26(1): 150-161.